

# Fibrous Polyethyleneimine-Functionalized Cellulose Materials for CO<sub>2</sub> Capture and Release

Marc P. Vocht, Patricija Tomasic, Ronald Beyer, Alexandra Müller, Ulrich Zuberbühler, Bernd Stürmer, Frank Hermanutz, and Michael R. Buchmeiser\*

**Poly(ethyleneimine) (PEI) immobilized on support materials are valuable alternatives to aqueous amine solutions for carbon dioxide (CO<sub>2</sub>) capture from the atmosphere since the thermal desorption of CO<sub>2</sub> from these materials usually requires less energy. Herein, fibrous PEI-functionalized carrier systems based on cellulose, cellulose tosylate (CT), and cellulose carbamate (CC) are described. Branched PEI is used for functionalization since higher CO<sub>2</sub> sorption capacities compared to linear PEIs can be achieved. Under wet conditions, a PEI-functionalized nonwoven material has a sorption capacity of 0.026 mg CO<sub>2</sub>/mg adsorbent; complete and reversible CO<sub>2</sub> desorption is accomplished at 80 °C.**

## 1. Introduction

Carbon dioxide (CO<sub>2</sub>) is a climate-damaging exhaust gas. It can, however, also be used as a resource for plastics or renewable fuels, and thus potentially replace fossil natural gas and crude oil. Adsorption of CO<sub>2</sub> from air is currently under consideration for combating climate change in several respects: it can reduce the amount of the greenhouse gas in the atmosphere, make it usable for the chemical industry and thus enable a reduction in future emissions. Therefore, it is necessary to identify methods for reducing and using the CO<sub>2</sub> being produced and emitted into the

atmosphere. Consequently, extensive research is devoted to the development of effective CO<sub>2</sub> adsorbents.<sup>[1–6]</sup> The most promising systems are based on immobilized amines.<sup>[7]</sup> These systems use the acid-base reaction of CO<sub>2</sub> with amine groups (chemisorption). Various types of amines have been used<sup>[10–13,2,8,9]</sup> and the corresponding materials can be produced easily and with low energy consumption.<sup>[14]</sup> However, different amines exhibit different thermal stability and CO<sub>2</sub> sorption and desorption behavior. The thermal stability of the adsorber material is critical, since it has a significant influence on the process temperature at which adsorbents can effectively

capture CO<sub>2</sub>.<sup>[2]</sup> Compared to low-molecular weight amines such as monoethanolamine (MEA), diethanolamine (DEA), triethanolamine (TEA), and tetraethylenepentamine (TEPA), polymeric amines such as poly(ethyleneimine) (PEI), have higher thermal stability, low vapor pressure and are thus ideal adsorbents for capturing CO<sub>2</sub>.<sup>[15,16]</sup> In addition, amine-based adsorbents are tolerant towards water since the adsorption of water is not in unfavorable competition with CO<sub>2</sub> adsorption, as is the case with other adsorbents such as zeolites and activated carbons.<sup>[17]</sup> Reversible reaction of CO<sub>2</sub> and amine-groups in the presence of H<sub>2</sub>O is comparably faster than without water.<sup>[18]</sup> Due to their high amino group content, molecules containing polyamines are more suitable as CO<sub>2</sub> adsorber materials than compounds with a low amino group content. Thirion et al. claimed that linear polymeric amines like PEI adsorb CO<sub>2</sub> by a so called “wrapping mechanism,” where the amine-CO<sub>2</sub> product is stabilized through multiple intermolecular H-bonding interactions.<sup>[19]</sup> Once immobilized, e.g. on silica, the stability of PEI depends on its molecular weight and the PEI type.<sup>[7]</sup> Chen et al. and Olah et al. showed that branched PEIs are particularly suitable for the synthesis of amine-based silica adsorbents, due to their large sorption capacities and high thermal stability.<sup>[11,20,7]</sup>


As for all amines, the binding of PEI is based on the selective reaction of the amine groups with CO<sub>2</sub>. However, different amine groups – primary, secondary, and tertiary – react under different conditions as shown in **Figure 1**.<sup>[16,21]</sup> The reaction of CO<sub>2</sub> with primary or secondary amines (Figure 1a,b) is usually described by a zwitterionic mechanism resulting in the formation of carbamates.<sup>[22]</sup> This reaction is possible under dry conditions at temperatures of ≈40 °C.<sup>[21]</sup> The CO<sub>2</sub> loading capacity for primary and secondary amines is in the range 0.5–1.0 mol of CO<sub>2</sub> per mol of amine, since a fraction of the carbamate species

M. P. Vocht, P. Tomasic, R. Beyer, A. Müller, F. Hermanutz,  
M. R. Buchmeiser

German Institutes of Textile and Fiber Research (DITF)  
Körschtalstr. 26, Denkendorf 73770, Germany  
E-mail: michael.buchmeiser@ipoc.uni-stuttgart.de

U. Zuberbühler, B. Stürmer  
Center for Solar Energy and Hydrogen Research Baden-Württemberg  
(ZSW)  
Meitnerstraße 1, Stuttgart 70563, Germany

M. R. Buchmeiser  
Chair of Macromolecular Compounds and Fiber Chemistry  
Institute of Polymer Chemistry (IPOC)  
University of Stuttgart  
Pfaffenwaldring 55, Stuttgart 70550, Germany

 The ORCID identification number(s) for the author(s) of this article can be found under <https://doi.org/10.1002/mame.202200093>

© 2022 The Authors. Macromolecular Materials and Engineering published by Wiley-VCH GmbH. This is an open access article under the terms of the Creative Commons Attribution License, which permits use, distribution and reproduction in any medium, provided the original work is properly cited.

DOI: 10.1002/mame.202200093

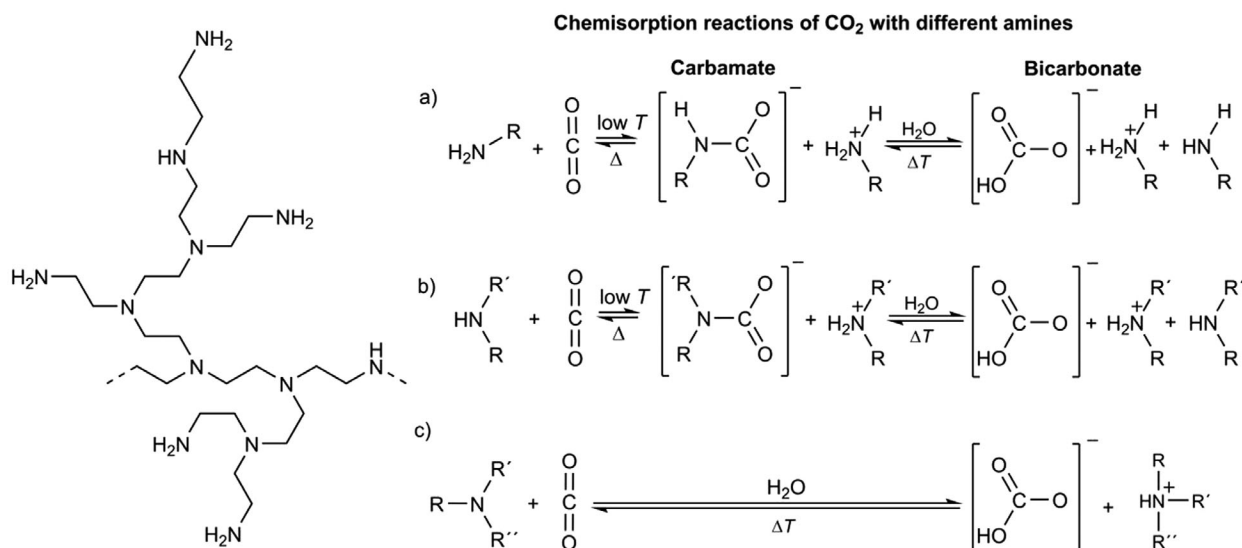


**Figure 1.** Representative structure of branched PEI and reactions of the amine groups with CO<sub>2</sub>/H<sub>2</sub>O.

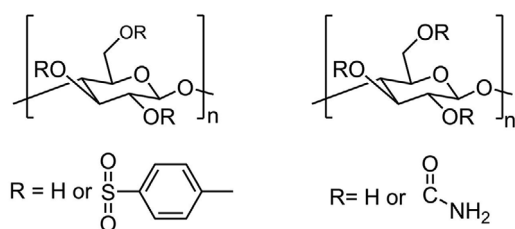


**Figure 2.** Chemical structure of cellulose tosylate (left) and cellulose carbamate (right).

is hydrolyzed to form hydrogen carbonates (bicarbonates). The reaction of tertiary amines with CO<sub>2</sub> (Figure 1c) is based on a base-catalyzed hydration of CO<sub>2</sub> to form hydrogen carbonate and can only be performed in the presence of water. The loading capacity of tertiary amines is  $\approx 1$  mol of CO<sub>2</sub> per mol of amine. Generally, the presence of water can significantly increase both CO<sub>2</sub> adsorption capacity and stability.<sup>[23,24]</sup> Apart from the CO<sub>2</sub> adsorption capacity, the development of a low-cost support material is important for any industrial application. An efficient and sustainable carrier system is cellulose, which has already been used in the form of amine-functionalized nanofibers for CO<sub>2</sub> adsorption.<sup>[25–29]</sup> However, these materials show comparably low adsorption capacities for CO<sub>2</sub>.<sup>[16]</sup> Here we report on the preparation of fibrous cellulose, cellulose tosylate (CT), and cellulose carbamate (CC) materials (Figure 2) and their use as carrier systems for PEI. The tosylate group in CT served as leaving group in the functionalization with branched PEI leading to a covalent attachment of PEI to the cellulose-based carrier.

## 2. Results and Discussion

### 2.1. Optimization of the Spinning System

The first step in the production of the carrier material was fiber spinning. However, in the case of cellulose and cellulose deriva-

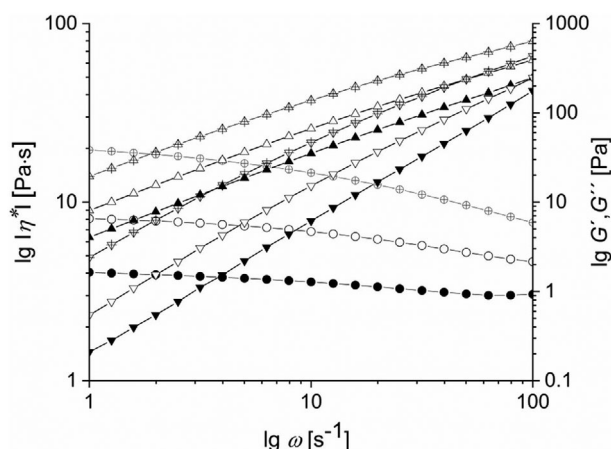


**Figure 3.** Flow curve of an 8 wt% CT/CC solution measured at 20 °C (symbols with lines), 40 °C (unfilled symbols) and 60 °C (filled symbols), complex viscosity  $|\eta^*|$  (●), storage  $G'$  (▼) and loss  $G''$  (▲) modulus.

tives, this is limited to a few solvents. Pure cellulose fibers are technically produced by the Lyocell or viscose process using *N*-morpholine-*N*-oxide or CS<sub>2</sub>/NaOH.<sup>[30]</sup> Another promising approach is the use of ionic liquids (ILs) as alternative solvents,<sup>[31]</sup> which offers access to fibers with outstanding properties.<sup>[32]</sup> Accordingly, a solution of 8 wt% of cellulose tosylate (CT) was prepared using [EMIM][Oct]. Unfortunately, the triflate group was found to be replaced by the octanoate moiety, rendering this approach unsuitable. Instead, LiCl (5.6 wt%) in DMAc had to be chosen. Pure cellulose as blend polymer was discarded due to its comparably low solubility in DMAc/LiCl. Instead, cellulose carbamate (CC) with a  $\text{DS}_{\text{carbamate}}$  of 0.3 was found to be a suitable carrier polymer. CC itself possessed good solubility in the solvent system. A solution of 8 wt% of polymers with a ratio of CT:CC of 1:3 was prepared. Results of the rheological experiments are shown in Figure 3. The flow behavior was measured at different temperatures (20, 40, and 60 °C). The solution showed shear thin-

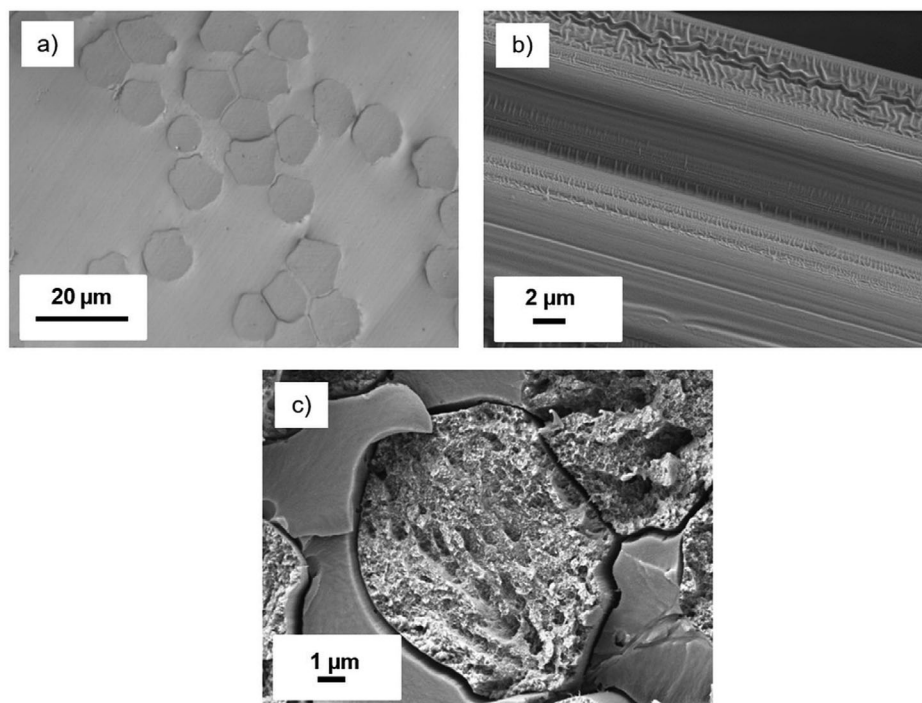


**Figure 4.** a) Light microscope image of the cross section, SEM images b) of the surface and c) of the fiber cross section.

ning behavior with zero-shear viscosities ( $\eta_0$ ) between 1 and 20 Pa s. The loss modulus ( $G''$ ) exceeded the storage module ( $G'$ ), resulting in a loss factor  $\delta > 1$ , indicating a viscoelastic behavior of the solution.

With the aid of a doctor blade a stable foil could be produced. Analysis of the blend foil by IR spectroscopy showed that the functional groups of both cellulose derivatives were present after coagulation. Thus, the carbamate bands were observed at 1702 and 1606  $\text{cm}^{-1}$ , respectively; the tosylate bands showed up at 1155, 823, and 663  $\text{cm}^{-1}$ , respectively. Elemental analysis revealed a sulfur content of 1%.

## 2.2. Fiber Spinning and Characterization of the Precursor Fibers

Based on the data outlined above, the dissolution process was scaled up and spinning trials were conducted as described in the Experimental Section. The process parameters and the fiber properties are summarized in Table S4 in the Supporting Information. The tenacity of the blend fibers was reduced compared to those of viscose or cellulosic fibers prepared by the IL process.<sup>[31,33]</sup> However, they were sufficiently stable enough to be processed into knitted fabrics and nonwovens. **Figure 4** depicts the microscope pictures and SEM images of both the surface and the cross-section of the resulting blend fibers, Figure S7 in the Supporting Information. The fibers showed an irregular geometry and a rough surface structure, both attributable to the wet spinning process. The rough structure of the fiber cross section was caused by sample preparation. No phase separation between the two cellulose derivatives could be detected.

Analysis of the blend fiber showed that in analogy to the blend foil both the carbamate (1702 and 1606  $\text{cm}^{-1}$ ) and tosylate group

**Table 1.** PEI materials produced, with details of the treatment parameters and the grafting efficiency (GE) for **C-PEI-1**.

Material	Material	Time/Temp.	Solvent/PEI concentration	GE [%]
<b>C-PEI-1</b>	blend fiber	2 h/ 59 °C	acetone/10 wt%	23
<b>C-PEI-2</b>	viscose nonwoven	2 h/ 59 °C	acetone/25 wt%	–

(1155, 823, and 663  $\text{cm}^{-1}$ ), Figure S6 (Supporting Information). Elemental analysis revealed a sulfur content of 1.2 wt%, similar to the results for the foil.

## 2.3. Functionalization with PEI

Both blend-fibers and a viscose nonwoven material were functionalized with PEI. Prior to functionalization, all materials were thoroughly washed to remove any finishing agent. Acetone was chosen as solvent to prevent structural loss of the nonwoven. By using water or other suitable solvents for PEI, the functionalized non-woven adhered and shrank, yielding a collapsed structure. Furthermore, acetone could not dissolve the blend fibers, instead causing a swelling, which was considered to be beneficial for functionalization. The PEI solution was then heated and mixed with the corresponding fiber material. After the reaction, all samples were washed with water at 40 °C for 1 h. Reaction conditions and the grafting efficiency calculated for 1 g of starting material are summarized in **Table 1**.

The nitrogen content of both **C-PEI-1** (13.1 wt%) and **C-PEI-2** (15.2 wt%) was  $\approx 85\%$  higher than the one of commercial PEI-cellulose (2.2 wt%), which demonstrates the attractiveness of this approach. The resulting materials were analyzed by elemental

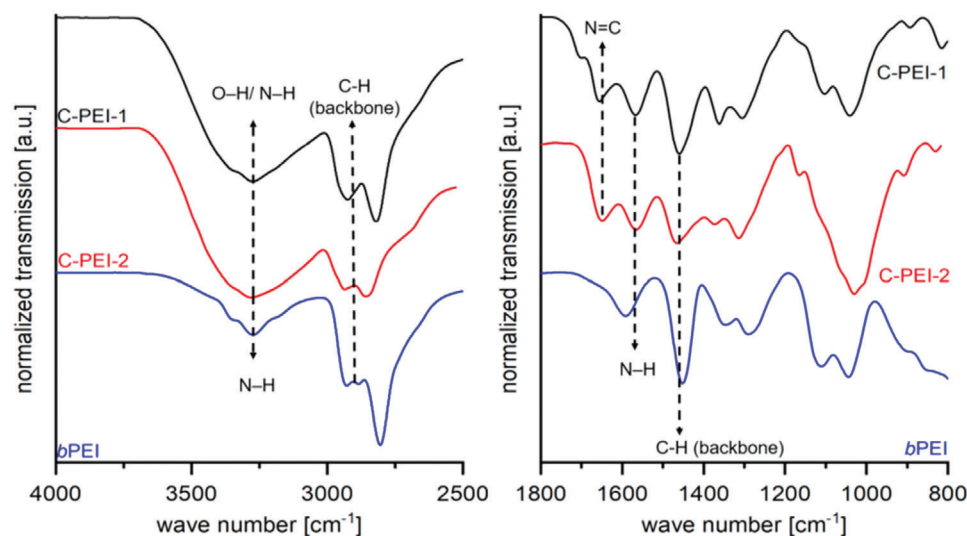


**Figure 5.** IR-spectra of C-PEI-1 (black), C-PEI-2 (red) and branched PEI (*b*PEI, blue); left: 4000–2500 cm<sup>-1</sup>, right: 1800–800 cm<sup>-1</sup>.

**Table 2.** CO<sub>2</sub> capture capacity under dry and humid conditions and H<sub>2</sub>O uptake.

Material	CO <sub>2</sub> -capture [mg CO <sub>2</sub> /mg sorbents]		H <sub>2</sub> O-uptake [wt%]
	dry conditions	humid conditions	
Lewatit	0.015	0.029	8.8
PEI-cellulose	no measurable CO <sub>2</sub> adsorption		
C-PEI-1	0.0039	0.010	27.2
C-PEI-2	0.0069	0.026	24.7

analysis and IR spectroscopy (Table S3, full spectra Figure S8 Supporting Information). All samples showed the characteristic amine bands 3260–3270 cm<sup>-1</sup> ( $\nu_{\text{N-H}}$  primary/secondary), the alkane bands 2800–2950 cm<sup>-1</sup> ( $\nu_{\text{C-H}}$  – alkanes), 1650–1550 cm<sup>-1</sup> ( $\delta_{\text{N-H}}$ ), 1460 cm<sup>-1</sup> ( $\delta_{\text{C-H}}$  – alkanes) after functionalization with PEI, **Figure 5**. A further band was observed at 1640–1690 cm<sup>-1</sup>. The band can be assigned to the stretching vibration of an imine group ( $\nu_{\text{C=N}}$  – imines), which is formed by a side reaction of acetone and PEI.<sup>[34,35]</sup>

## 2.4. CO<sub>2</sub> Capture and Release

As already outlined, the binding of CO<sub>2</sub> to PEI is based on the reaction of the amino groups with CO<sub>2</sub>. PEI possesses primary, secondary as well as tertiary amines. Since tertiary amines can only bind CO<sub>2</sub> in the presence of water, the CO<sub>2</sub> sorption ability of the prepared materials was tested under both, humid and dry conditions. Results were compared to those obtained with Lewatit, a macroporous, divinylbenzene-crosslinked anion exchanger, which is currently among the most promising candidates for CO<sub>2</sub> capture. Results of the CO<sub>2</sub> adsorption capacities measurements are summarized in ref. [24, 28].

**Table 2.** The corresponding TGA diagrams are given in Figure S9 (Supporting Information). The commercial PEI-cellulose sample did not adsorb any significant amounts of CO<sub>2</sub> due to

the low amine group content of the sample. Although under humid conditions the total mass of commercial PEI-cellulose increased to a stable value during the adsorption step, no CO<sub>2</sub> signal was observed in the subsequent desorption step. In other words, only water was adsorbed during the adsorption step. Under dry conditions, neither a significant mass gain nor CO<sub>2</sub> desorption was achieved. **Lewatit**, which has only primary amino groups, had a higher CO<sub>2</sub> adsorption capacity in the wet state (0.029 mg CO<sub>2</sub>/ mg sorbents) compared to the dry state (0.015 mg CO<sub>2</sub>/ mg sorbents). Higher CO<sub>2</sub> uptake under humid conditions is due to the fact that only one amino group is necessary to capture a molecule of CO<sub>2</sub>, while two amino groups are necessary under dry conditions.<sup>[36]</sup> Furthermore, the higher adsorption capacity can be attributed to the strong swelling of the material under wet conditions, which renders the amine groups more accessible but at the same time increases the back pressure in the corresponding Lewatit-filled columns. The presence of water is also advantageous as it stabilizes the PEI-based sorbent by inhibiting the formation of urea species and avoiding CO<sub>2</sub>-induced degradation.<sup>[28,6]</sup> A similar trend was observed for the PEI-functionalized materials **C-PEI-1** and **C-PEI-2**, respectively. With these materials, the increased CO<sub>2</sub> adsorption-capacity under humid conditions is also, at least in part, attributable to the tertiary amino groups of the PEI molecule, which require water to form the corresponding hydrogen carbonate anions. In addition, as is the case with Lewatit, the adsorption capacity is also influenced by the surface area of the adsorption material. While under wet conditions **C-PEI-1** showed an adsorption capacity of 0.010 mg CO<sub>2</sub>/mg sorbent, **C-PEI-2** showed an adsorption capacity of 0.026 mg CO<sub>2</sub>/ mg sorbent, which is similar to the one of Lewatit. We surmise that the higher sorption capacity of **C-PEI-2** for CO<sub>2</sub> is caused by an interplay of various factors, such as the open structure of the nonwoven, allowing for a fast diffusion of CO<sub>2</sub> to the amine sites, high PEI-loading on the surface, providing sufficient amine sites for CO<sub>2</sub> adsorption, and humid conditions to fully unlock the potential of PEI-based sorbents.<sup>[24,28]</sup>

Water uptake of the measured samples was in all cases significantly higher than the CO<sub>2</sub> adsorption capacity. This can be



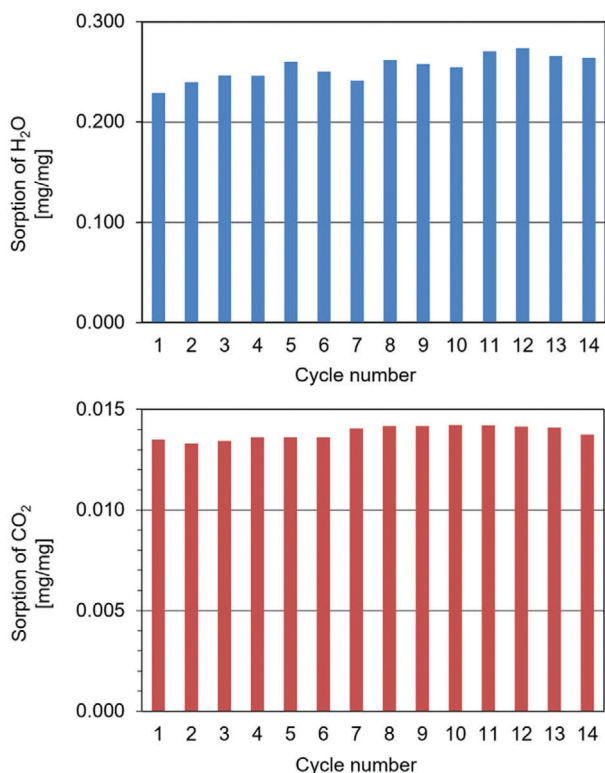


**Figure 6.** Sorption values [mg/mg] of H<sub>2</sub>O (top) and CO<sub>2</sub> (bottom) for each cycle.

attributed to the relatively low concentration of CO<sub>2</sub> (360 ppm) compared to water (50% relative humidity at 25 °C) in the synthetic air used, and to the general hygroscopic nature of cellulosic materials.<sup>[37]</sup>

### 2.5. Cycle Performance and Kinetic Measurements

The cycle performance of an adsorption material is important for practical application as it directly affects the costs for CO<sub>2</sub> adsorption. As **C-PEI-2** showed the highest CO<sub>2</sub> capture capacity, the cycle performance of this material was tested under humid conditions, Figure S10 (Supporting Information). The material retained its cycle performance after 14 consecutive experiments. Both H<sub>2</sub>O and CO<sub>2</sub> adsorption proceeded without any hysteresis indicating that there was no irreversible binding. For practical reason, the adsorption time was reduced during the cycle test, which resulted in a reduction of the adsorbed amounts of both, H<sub>2</sub>O and CO<sub>2</sub>, **Figure 6**.

The binary system (H<sub>2</sub>O/CO<sub>2</sub>) makes the determination of adsorption isotherms difficult. However, to fully characterize

the PEI-functionalized adsorbents, we calculated the adsorption rate ( $k$ ), for both H<sub>2</sub>O and CO<sub>2</sub> assuming (at least initial) simultaneous adsorption, as the change of mass over the adsorption time.<sup>[38]</sup>

$$\frac{dm}{dt} = k \quad (1)$$

It was observed that the mass increase changed during the adsorption measurements. Therefore, two adsorption rates  $k_1$ ,  $k_2$  were calculated by adding two tangents to the graph. Tangent 1 ( $k_1$ ) was applied for the first 45 min of the adsorption time, while tangent 2 ( $k_2$ ) was applied for the last 4 h. The calculated values are an average of the 14 consecutive cycles, **Table 3**. Generally,  $k_1$  had a higher value than  $k_2$ , which indicates a faster adsorption at the beginning. This behavior is typical for the adsorption of gases and gas mixtures,<sup>[24,39,40]</sup> since the material is initially not loaded with CO<sub>2</sub> and contains many free amine sites. It was also observed that the adsorption rate did not change over the time. This demonstrates a promising stability and reliability as a CO<sub>2</sub>-capture material.

### 3. Conclusions

Carrier materials based on cellulose, cellulose tosylate (CT) and cellulose carbamate (CC) have been synthesized and used for the preparation of a blend fiber system based on CT/CC. The resulting fibers had a tensile strength of 200 MPa. The average Young's modulus was 11 GPa and the elongation at break was 10%. Due to these mechanical properties, it was possible to process these fibers into a knitted fabric. The blend fibers as well as a viscose non-woven were modified with branched poly(ethylenimine) (PEI). The successful impregnation of carrier materials was confirmed by elemental analysis and infrared spectroscopy. The capturing of CO<sub>2</sub> was evaluated under dry and wet conditions. Sorption capacities were substantially higher under wet adsorption conditions due to the nature of the PEI, which contains many tertiary amine groups. Compared to a commercial Lewatit system, the nonwoven sample had a similar CO<sub>2</sub> adsorption capacity of 0.026 mg CO<sub>2</sub>/mg of sorbent material. Clearly, nonwoven based systems have the advantage that they possess an open structure, which in turn requires a lower pressure to bring them into contact with CO<sub>2</sub>. The stability of **C-PEI-2** under humid conditions was experimentally shown for 14 consecutive adsorption-desorption cycles. The material showed a stable CO<sub>2</sub> adsorption capability over all cycles. However, as the experimental run time progressed, the adsorption rate decreased. This behavior will be investigated further in the future as an optimal time/CO<sub>2</sub> balance is a key figure for any industrial application. It should be noted that the chosen adsorption and desorption conditions were optimized for laboratory STA measurements. For

**Table 3.** CO<sub>2</sub> capture capacity under humid conditions and H<sub>2</sub>O uptake.

material	Adsorption rate as a function of time		CO <sub>2</sub> -capture	H <sub>2</sub> O-uptake
	$k_1$ [mg h <sup>-1</sup> ]	$k_2$ [mg h <sup>-1</sup> ]	[mg CO <sub>2</sub> /mg sorbents]	[wt%]
<b>C-PEI-2</b>	14.00 ± 0.98	1.54 ± 0.18	0.014 ±	25.4 ± 1.2

future experiments regarding the practical application of the materials, both adsorption and desorption conditions, e.g., a combination of increased temperature and reduced pressure, need to be adjusted. On one hand, short cycle times maximize the amount of CO<sub>2</sub> captured by the adsorbent material per time, which can reduce costs. On the other hand, longer cycles favor high CO<sub>2</sub> loading and minimizes the required desorption energy. The optimal period represents a compromise between these two factors.

#### 4. Experimental Section

**Materials:** Two different cellulose materials were used: eucalyptus sulfite pulp (DP = 560, Sappi Saiccor) and alkali cellulose (DP<sub>EWN</sub> 388, 31.3% cellulose, 17% NaOH). 1-Ethyl-3-methylimidazolium octanoate ([EMIM][Oct]) was provided by BASF SE. Commercial ion exchanger materials, i.e., Lewatit VP OC 1065 (Sigma) and a PEI-cellulose (particle size < 74 μm, capacity = 1.1 meq g<sup>-1</sup>, Sigma), were used as reference materials for CO<sub>2</sub> capture measurements. All used chemicals are listed in Table S1 in the Supporting Information.

**Methods:** Elemental analyses (EA) were carried out using a Perkin Elmer Analyzer 240. The degree of substitution (DS) of the prepared cellulose derivatives was determined by EA. DS<sub>tosylate</sub> was determined via the sulfur content and DS<sub>carbamate</sub> was calculated via the nitrogen content

$$DS_{\text{tosylate}} = \frac{\frac{S[\%]}{100\%} \cdot M_{\text{AGU}} \times M_S}{M_{\text{Cl}} \times M_S - \frac{S[\%]}{100\%} \cdot M_{\text{Cl}} \times M_{\text{Tosyl}} - \frac{Cl[\%]}{100\%} \times M_{\text{Cl}} \times M_S} \quad (2)$$

IR spectra of the materials were recorded on a Perkin Elmer 2000 Fourier-transform infrared spectrometer (FTIR). Rheological measurements were performed on an Anton Paar MCR 301 rheometer equipped with a Peltier temperature-control system and parallel-plate geometry. The plates' diameter was 25 mm; the gap was 1 mm. Dynamic oscillatory experiments were accomplished with shear rates of 1–100 s<sup>-1</sup> and a deformation of 10% at temperatures between 100 and 50 °C. Storage and loss modulus (*G'* and *G''*) and the complex viscosity (*η\**) were determined. With the principle of frequency–temperature superposition, master curves were obtained. The zero-shear viscosity *η*<sub>0</sub> was calculated using the Carreau–Gahleitner model.<sup>[41]</sup> Fiber materials were characterized according to EN ISO 5079. The fineness (d<sub>tex</sub>), tensile strength (MPa), elongation at break (%), and Young's modulus (MPa) were measured using a Favimat from Textechno. Fiber samples were conditioned prior to the measurement (20 °C, 60% humidity). Properties are calculated on the basis of 20 individual measurements. A Zeiss Auriga field emission scanning electron microscope was used for scanning electron microscopy (SEM). Samples were sputtered with Pt/Pd. CO<sub>2</sub> adsorption measurements were carried out at the ZSW Stuttgart using a simultaneous thermal analysis system (STA 409CD, Netzsch). Cellulose-based samples were heated under nitrogen at 80 °C, Lewatit was heated to 100 °C for 0.5 h before adsorption. CO<sub>2</sub>-adsorption was accomplished at 25 °C for 10 h using synthetic air containing 360 ppm of CO<sub>2</sub>. Synthetic air containing 400 ppm of CO<sub>2</sub> or more could not be applied because the sensitive STA scale required a protective nitrogen flow diluting the air. For the adsorption tests under humid conditions the relative humidity was 50%. After each adsorption step, desorption of CO<sub>2</sub> was carried out at 80 °C and at 100 °C (Lewatit) in a nitrogen atmosphere for 1 h. Thereby, the adsorbed amount of CO<sub>2</sub> was determined at the desorption step using a continuous gas analyzer X-STREAM Enhanced XEGP (Emerson). For all measurements a gas flow of 200 mL min<sup>-1</sup> was used. The cyclic performance of CO<sub>2</sub> adsorption under humid conditions was studied using the same experimental setup as described above. Adsorption was accomplished at 25 °C; desorption was carried out at 80 °C. Mass values during adsorption were normalized; the measured mass after preconditioning was set to 0 and the highest measured mass during adsorption was set to 1.

**Synthesis and Material Preparation:** Cellulose tosylate (CT) synthesis was carried out according to Rahn et al.<sup>[42]</sup> 40 g of cellulose (DP<sub>EWN</sub> = 560) were suspended in 1000 mL of *N,N*-dimethylacetamide (DMAc) under N<sub>2</sub> and stirred at 160 °C for 1 h. Subsequently, about 90 mL DMAc were removed by distillation at 180 °C. After the mixture had reached 100 °C, 80 g of LiCl (anhydrous) were added and cooled to room temperature while stirring. The solution was then transferred to a double jacket stirred reactor. 64 mL triethylamine (TEA) dissolved in 46 mL DMAc were added dropwise at room temperature. Then, the solution was cooled to 8 °C. Next, a solution of 46 g of *p*-toluenesulfonic acid chloride (TosCl) in 68 mL DMAc was added. The reaction mixture was stirred for 24 h at 8 °C, then poured into ice water (10 L) and slipped off. Washing was accomplished with 25 L demineralized water and 5 L ethanol. The resulting solid was dried in air. The crude solid was suspended in 2 L acetone, precipitated in 6 L of demineralized water and dried in vacuo at 60 °C. The product was ground before the dissolution tests. Yield: 90%, elemental analysis C: 48.1%, H: 5.1%, S: 9.7%, degree of substitution DS<sub>tosylate</sub> = 0.8 (based on sulfur analysis).

Cellulose carbamate (CC) was prepared according to the literature using alkali cellulose (DP<sub>EWN</sub> = 388, 31.3% cellulose, 17% NaOH).<sup>[43]</sup> 3.99 kg of the alkali cellulose were washed with 18 L methanol. 2.5 kg urea were added to a mixing kneader and molten at 148 °C. Within 35 min the cellulose was added. At 133 °C the mixture was allowed to react for 1.5 h under nitrogen atmosphere (1.5 bar). Afterwards, the mixture was mixed with 15 L of warm water and 30 L of cold water. The product was pressed and dried in air. Yield: 85%, elemental analysis C: 40.3%, H: 2.7%, N: 2.7%, degree of substitution DS<sub>carbamate</sub> = 0.3 (based on nitrogen analysis).

For foil preparation and fiber spinning, solutions were prepared in a laboratory blender (Waring) with a shear rate of 22 000 rpm. CT was mixed with [EMIM][Oct] to form a homogeneous suspension at room temperature for 60 s. The mixture was heated to 80 °C and the polymer dissolved within 1 h. For degassing, the mixture was stored in a vacuum oven at 60 °C and 100 mbar for 12 h. Blend solutions of CC and CT in DMAc/LiCl were prepared in two steps. First, CC was swollen in water for 12 h. Afterwards, water was exchanged by DMAc; this procedure was repeated twice. A DMAc/LiCl solution (with 5.6 wt% of LiCl) was added to pretreated CC and CT while stirring. The resulting mixture was refrigerated overnight. After the refrigeration step, the solution was filtered with the aid of a Karl Kurt Juchheim Laborgeräte GmbH laboratory-scale filtration vessel with a metallic tissue (mesh size: 50 μm) at 50 °C and 1 bar. The prepared solution had a cellulose derivative content of 8 wt% (ratio CT:CC = 1:3).

Cellulose derivative solutions in [EMIM][Oct] and DMAc/LiCl were cast into foils of 200 μm thickness with the aid of a film applicator (doctor blade). Foils were coagulated in a bath of demineralized water for 1 h. The coagulation medium was renewed twice and the foils were kept overnight in water to remove residual ionic liquid (IL) and DMAc/LiCl. Films were dried in air (Figures S3 and S5, Supporting Information).

Multi-filament fiber spinning was performed on a laboratory-scale wet spinning device. The spinning dope was passed through a filter with a mesh size of 0.043 mm. The extruder was heated and delivered the spinning dope to the multihole spinneret into a coagulation bath (DMAc/water, 30/70). The fibers were wound around godets under concomitant stretching before passing them through washing baths, two washing godets and a finishing bath. Before being wound onto a bobbin, they were dried on a heated godet (80 °C). The fibers were processed into a knitted fabric on a circular knitting machine (Harry Lucas) at a speed of 8 m h<sup>-1</sup>.

Two PEI functionalized materials were prepared, **C-PEI-1** and **C-PEI-2**. Prior to functionalization, the starting materials were washed with water for 2 h at 50 °C and dried at 100 mbar. For **C-PEI-1**, a solution of PEI (3 g) in acetone (27 g) was freshly prepared and heated to 50 °C. Then 1.0 g of the blend fibers (CT:CC = 1:3) were added and the reaction was allowed to proceed for 2 h. The reaction is outlined in Figure S2 in the Supporting Information. For **C-PEI-2**, nonwoven viscose fibers served as starting material, which were treated with 30 g of a 25 wt% solution of PEI in acetone for 2 h at 50 °C. After the reaction, all samples were separated and flushed with demineralized water and acetone. Subsequently, the sample was placed in demineralized water at 40 °C for 1 h and then dried at 100 mbar at 40 °C.

The grafting efficiency (GE, %) for **C-PEI-1** can be calculated from Equation 3<sup>[44]</sup>

$$GE = 100 \times \frac{(m_{\text{tosylate per g blend fiber}} - m_{\text{tosylate per g blend fiber in C-PEI-1}})}{m_{\text{tosylate per g blend fiber}}} \% \quad (3)$$

With  $m_{\text{tosylate per g blend fiber}}$  and  $m_{\text{tosylate per g blend fiber in C-PEI}}$  being the masses tosylate per gram unmodified blend fiber and per gram blend fiber in **C-PEI-1**, respectively.

## Supporting Information

Supporting Information is available from the Wiley Online Library or from the author.

## Acknowledgements

The authors wish to thank the Federal Ministry of Education and Research for financing the CORAL-project (FKZ 033RC005A) within the CO2Plus program. M.R.B. and M.P.V. thank the Vector Stiftung (project P2021-0038) for Financial Support. Furthermore, the authors would like to thank Dipl.-Geol. U. Hageroth and S. Henzler for SEM measurements.

Open Access funding enabled and organized by Projekt DEAL.

## Data Availability Statement

The data that support the findings of this study are available from the corresponding author upon reasonable request.

## Conflict of Interest

The authors declare no conflict of interest.

## Keywords

carbon dioxide, cellulose, fiber spinning, immobilization, polyethyleneimine

Received: February 9, 2022

Revised: March 28, 2022

Published online: May 2, 2022

- [1] A. L. Chaffee, G. P. Knowles, Z. Liang, J. Zhang, P. Xiao, P. A. Webley, *Int. J. Greenhouse Gas Control* **2007**, *1*, 11.
- [2] A. M. Varghese, G. N. Karanikolos, *Int. J. Greenhouse Gas Control* **2020**, *96*, 103005.
- [3] F. Akhtar, L. Andersson, N. Keshavarzi, L. Bergström, *Appl. Energy* **2012**, *97*, 289.
- [4] M. G. Plaza, A. S. González, C. Pevida, J. J. Pis, F. Rubiera, *Appl. Energy* **2012**, *99*, 272.
- [5] X. Xu, C. Song, J. M. Andresen, B. G. Miller, A. W. Scaroni, *Energy Fuels* **2002**, *16*, 1463.
- [6] A. Sayari, Y. Belmabkhout, *J. Am. Chem. Soc.* **2010**, *132*, 6312.
- [7] K. Li, J. Jiang, F. Yan, S. Tian, X. Chen, *Appl. Energy* **2014**, *136*, 750.
- [8] P. J. E. Harlick, A. Sayari, *Ind. Eng. Chem. Res.* **2007**, *46*, 446.
- [9] D. S. Mebane, J. D. Kress, C. B. Storlie, D. J. Fauth, M. L. Gray, K. Li, *Am. J. Phys. Chem.* **2013**, *117*, 26617.
- [10] R. Sanz, G. Calleja, A. Arencibia, E. S. Sanz-Pérez, *Energy Fuels* **2013**, *27*, 7637.
- [11] A. Goeppert, S. Meth, G. K. S. Prakash, G. A. Olah, *Energy Environ. Sci.* **2010**, *3*, 1949.
- [12] S. Choi, M. L. Gray, C. W. Jones, *ChemSusChem* **2011**, *4*, 628.
- [13] C.-H. Yu, C.-H. Huang, C.-S. Tan, *Aerosol Air Qual. Res.* **2012**, *12*, 745.
- [14] G. Qi, L. Fu, B. H. Choi, E. P. Giannelis, *Energy Environ. Sci.* **2012**, *5*, 7368.
- [15] A. n Zhao, A. Samanta, P. Sarkar, R. Gupta, *Ind. Eng. Chem. Res.* **2013**, *52*, 6480.
- [16] X. Shen, H. Du, R. H. Mullins, R. R. Kommalapati, *Energy Technol.* **2017**, *5*, 822.
- [17] Y. Belmabkhout, R. Serna-Guerrero, A. Sayari, *Adsorption* **2011**, *17*, 395.
- [18] H. Zhang, H. Tian, J. Zhang, R. Guo, X. Li, *Int. J. Greenhouse Gas Control* **2018**, *78*, 85.
- [19] D. Thirion, V. Rozyyev, J. Park, J. Byun, Y. Jung, M. Atilhan, C. T. Yavuz, *Phys. Chem. Chem. Phys.* **2016**, *18*, 14177.
- [20] Y. Yu, J. Wang, Y. Wang, W. Pan, C. Liu, P. Liu, L. Liang, C. Xu, Y. Liu, *J. Ind. Eng. Chem.* **2020**, *83*, 20.
- [21] D. M. D'alessandro, B. Smit, J. R. Long, *Angew. Chem., Int. Ed.* **2010**, *49*, 6058.
- [22] P. D. Vaidya, E. Y. Kenig, *Chem. Eng. Technol.* **2007**, *30*, 1467.
- [23] N. Hiyoshi, K. Yogo, T. Yashima, *Microporous Mesoporous Mater.* **2005**, *84*, 357.
- [24] C. Gebald, J. A. Wurzbacher, A. Borgschulte, T. Zimmermann, A. Steinfeld, *Environ. Sci. Technol.* **2014**, *48*, 2497.
- [25] C. Gerald, T. Zimmermann, P. Tingaut (invs.), Porous adsorbent structure for adsorption of CO2 from a gas mixture, AU2017204830A1, Eidgenössische Materialprüfungs- und Forschungsanstalt EMPA, 2019.
- [26] C. Gebald, N. Piotowski, T. Rüesch, J. A. Wurzbacher (invs.), Low pressure drop structure of particle adsorbent bed for adsorption gas separation process, US9751039B2, Climeworks AG, 2017.
- [27] E. R. Monazam, R. W. Breault, D. J. Fauth, L. J. Shadle, S. Bayham, *Ind. Eng. Chem. Res.* **2017**, *56*, 9054.
- [28] C. Gebald, J. A. Wurzbacher, P. Tingaut, A. Steinfeld, *Environ. Sci. Technol.* **2013**, *47*, 10063.
- [29] L. Riva, A. Fiorati, C. Punta, *Materials* **2021**, *14*, 473.
- [30] K. Brederick, F. Hermanutz, *Rev. Prog. Color.* **2008**, *35*, 59.
- [31] F. Hermanutz, M. P. Vocht, N. Panzier, M. R. Buchmeiser, *Macromol. Mater. Eng.* **2018**, *304*, 1800450.
- [32] J. M. Spörl, A. Ota, S. Son, K. Massonne, F. Hermanutz, M. R. Buchmeiser, *Mater. Today Commun.* **2016**, *7*, 1.
- [33] F. Gähr, F. Hermanutz, *Melliand Textilber.* **2002**, *83*, 149.
- [34] T. Gharbi, G. Herlem, *In Biosensors – Emerging Materials and Applications* (Ed.: Serra P. A.), Vol. 1, IntechOpen, London, UK **2011**, p. 179.
- [35] Q. Zhao, Z. He, Y. Jiang, Z. Yuan, H. Wu, C. Su, H. Tai, *Front. Mater.* **2019**, *5*, 82.
- [36] H. Sehaqui, M. E. Gález, V. Becatinni, Y. i Cheng Ng, A. Steinfeld, T. Zimmermann, P. Tingaut, *Environ. Sci. Technol.* **2015**, *49*, 3167.
- [37] T. H. Mokhothu, M. J. John, *Carbohydr. Polym.* **2015**, *131*, 337.
- [38] C. Gebald, J. A. Wurzbacher, P. Tingaut, T. Zimmermann, A. Steinfeld, *Environ. Sci. Technol.* **2011**, *45*, 9101.
- [39] C. Wang, S. Okubayashi, *Carbohydr. Polym.* **2019**, *225*, 115248.
- [40] S. García, J. J. Pis, F. Rubiera, C. Pevida, *Langmuir* **2013**, *29*, 6042.
- [41] M. Gahleitner, R. Sobczak, *Kunststoffe -German Plastics* **1989**, *79*, 1213.
- [42] K. Rahn, M. Diamantoglou, D. Klemm, H. Berghmans, T. Heinze, *Angew. Makromol. Chem.* **1996**, *238*, 143.
- [43] F. Hermanutz, W. Oppermann (invs.), Production of Cellulose carbamate from Cellulose, DE1996135707, Deutsche Institute für Textil und Faserforschung 1998.
- [44] M. M. Fares, A. S. El-Faqeeh, M. E. Osman, *J. Polym. Res.* **2003**, *10*, 119.